Electron Transport through a Molecular Conductor with Center-of-Mass Motion

K. A. Al-Hassanieh,[1,2] C. A. Büsser,[1] G. B. Martins,[3] and E. Dagotto[1]

[1]*Condensed Matter Sciences Division, Oak Ridge National Laboratory, Oak Ridge, Tennessee 37831, USA
and Department of Physics, University of Tennessee, Knoxville, Tennessee 37996, USA*
[2]*National High Magnetic Field Laboratory and Department of Physics, Florida State University, Tallahassee, Florida 32306, USA*
[3]*Department of Physics, Oakland University, Rochester, Michigan 48309, USA*

The linear conductance of a molecular conductor oscillating between two metallic leads is investigated numerically both for Hubbard interacting and noninteracting electrons. The molecule-leads tunneling barriers depend on the molecule displacement from its equilibrium position. The results present an interesting interference which leads to a conductance dip at the electron-hole symmetry point that could be experimentally observable. It is shown that this dip is caused by the destructive interference between the purely electronic and phonon-assisted tunneling channels, which are found to carry opposite phases. When an internal vibrational mode is also active, the electron-hole symmetry is broken but a Fano-like interference is still observed.

PACS numbers: 73.63.−b, 71.27.+a, 72.10.−d, 85.65.+h

Molecular electronics has received much attention in the past decade, particularly since it became possible to fabricate devices in which the active element is a single molecule [1,2]. A fundamental property of molecular conductors is their discrete electronic spectrum. Although the weak coupling of the molecule to the two metallic electrodes leads to the broadening of the molecular energy levels, their discrete nature is maintained. Because of the small size of these molecules, electronic correlations are dominant and they lead to interesting many-body effects, such as the Coulomb blockade and Kondo resonance [3]. These effects have been observed experimentally in molecular conductors [4] and other nanostructures [5]. Another interesting property of molecules is their flexible nature. They have an intrinsic spectrum of internal vibrational modes and, when coupled to the electrodes, some molecules acquire external vibrational modes as well. The excitation of one or more of these modes modulates the electronic energy levels and tunneling barriers between the molecule and the electrodes or between different parts of the molecule, thus changing the molecular transport properties. These vibrational effects have been observed in a number of recent experiments [6,7] and have been the subject of considerable theoretical investigation [8].

In this work, we study the zero bias conductance of a molecular conductor model with one relevant electronic energy level, both with interacting and noninteracting electrons. The molecule is allowed to oscillate between the two electrodes. This center-of-mass (c.m.) vibrational mode is treated quantum mechanically and leads to an asymmetric modulation of the molecule-leads tunneling barriers. The vibrational excitation is also coupled to the charge on the molecule. This is due to the fact that the chemical bonds inside the molecule and the molecule-electrode bonds depend in general on the molecule's charge. The results show an interesting and unexpected conductance cancellation when an odd number of electrons occupy the mole-

cule. It is discussed below that this cancellation is due to the destructive interference between the purely electronic and phonon-assisted tunneling channels, which are found to carry opposite phases [9]. In this case both channels are elastic. The phonons are virtual, not thermal.

Figure 1 schematically depicts the system analyzed in this work. The molecule can oscillate between the source and drain electrodes, thus modulating the tunneling barriers. In our calculations, this modulation and the electron-vibration coupling are expanded up to the linear term [10,11]. The electronic part of the system is modeled using the Anderson impurity Hamiltonian. The total Hamiltonian can be written as $\hat{H} = \hat{H}_M + \hat{H}_{\text{leads}} + \hat{H}_{\text{M−leads}}$, where $\hat{H}_M$ is the Hamiltonian of the molecule,

$$\hat{H}_M = V_g \hat{n}_d + U \hat{n}_{d\uparrow} \hat{n}_{d\downarrow} + \lambda(1 - \hat{n}_d)(a + a^\dagger) + \omega_0 a^\dagger a.$$
(1)

The first term represents the energy of the relevant molecular orbital controlled by the gate voltage, the second term represents the Coulomb repulsion between the electrons occupying the molecular orbital, the third term couples the vibrational excitation to the net charge on the molecule ($a^\dagger$ and a are the phonon operators), and the fourth term represents the vibrational energy. $\hat{H}_{\text{leads}}$ describes the two leads modeled here as semi-infinite ideal chains, $\hat{H}_{\text{leads}} = -t \sum_{i\sigma}(c_{li\sigma}^\dagger c_{li+1\sigma} + c_{ri\sigma}^\dagger c_{ri+1\sigma} + \text{H.c.})$,
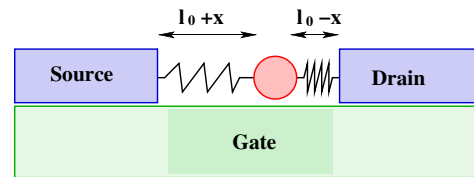

FIG. 1 (color online). A schematic of the system studied in this Letter. The molecule can oscillate between the two leads, thus modulating the tunneling barriers.

where $c_{li\sigma}^{\dagger}$ ($c_{ri\sigma}^{\dagger}$) creates an electron with spin σ at site i in the left (right) lead. t is the hopping amplitude in the leads and the energy scale ($t = 1$). $\hat{H}_{M-\text{leads}}$ connects the molecule to the leads,

$$\hat{H}_{M-\text{leads}} = t'[1 - \alpha(a + a^{\dagger})]\sum_{\sigma}(d_{\sigma}^{\dagger}c_{l0\sigma} + \text{H.c.})$$

$$+ t'[1 + \alpha(a + a^{\dagger})]\sum_{\sigma}(d_{\sigma}^{\dagger}c_{r0\sigma} + \text{H.c.}), \quad (2)$$

where $d_{\sigma}^{\dagger}$ creates an electron with spin σ in the molecule, t' is the hopping parameter between the molecule and the first site of each lead, and α is a parameter that carries the dependence of t' on the molecule displacement from its equilibrium position $\hat{x}$ (note the opposite signs in this dependence for the two leads). This displacement can be written in terms of the phonon operators as $\hat{x} = (a + a^{\dagger})$. The total Hamiltonian is invariant under the particle hole and $(a \rightarrow -a)$ transformation. In the results shown, unless otherwise stated the following set of parameters was used: $U = 1.0$, $t' = 0.2$, $\omega_0 = 0.2$, while λ and α were varied [12]. The value of ω_0 was fixed since its increase or decrease would simply produce the opposite effect of increasing or decreasing λ and/or α.

Using the Keldysh formalism [13], the zero bias and zero temperature conductance can be written as $G = \frac{2e^2}{h}|t^2 G_{\text{lr}}(\epsilon_F)|^2[\rho(\epsilon_F)]^2$, where G_{lr} is the Green function that propagates an electron from the left to the right lead and $\rho(\epsilon_F)$ is the density of states in the leads at the Fermi level. Note that at zero bias only elastic processes can be observed. The Green functions are calculated using exact diagonalization supplemented by a Dyson equation embedding procedure (ED + DE) [14].

It is useful to start by studying briefly the model when the tunnel barriers do not depend on the vibrational excitation ($\alpha = 0$). This was previously studied using numerical renormalization group (NRG) techniques [15]. In this case, the model can be mapped into an effective electronic Hamiltonian with renormalized parameters [$\tilde{U} = U - 2\lambda^2/\omega_0$, $\tilde{V}_g = V_g + \lambda^2/\omega_0$, and $\tilde{t}' \propto t' \exp(\frac{-\lambda^2}{2\omega_0^2})$] [15,16]. Figures 2(a) and 2(b) show the results in the interacting electrons case obtained using ED + DE and NRG, respectively. For weak electron-phonon coupling, the standard Kondo resonance is obtained with renormalized parameters. For strong electron-phonon coupling, the "charge Kondo effect" is obtained. Note that the results obtained using ED + DE are very similar to the NRG results, clearly capturing the essence of the problem. Since NRG methods cannot be applied to the c.m. oscillations studied here, and ED + DE appears equally accurate, the results presented below were obtained using this last technique.

Figure 3 contains the main results of this work. Figure 3(a) shows the conductance in the interacting electrons' case. For $\alpha = 0$, the conductance simply shows a Kondo resonance peak with reduced width. However, when
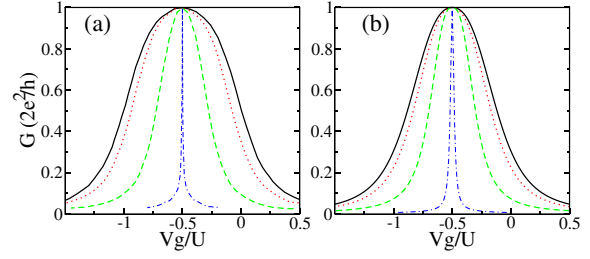

FIG. 2 (color online). (a) NRG and (b) ED + DE results for G as a function of V_g in the Kondo regime for $\alpha = 0$ and increasing λ ($\lambda/\omega_0 = 0.0, 0.4, 0.8$, and 1.2).

$\alpha \neq 0$, a conductance *dip* is obtained when an odd number of electrons occupy the molecule. Figure 3(b) provides the average occupation $\langle n_d \rangle$ of the molecular orbital where it can be clearly seen that the charging behavior is almost the same in both cases. Note that for $\alpha \neq 0$, the usual Friedel sum rule [17] $G = \frac{2e^2}{h}\sin^2(\frac{\pi}{2}\langle n_d\rangle)$ is not satisfied and this can be an indication of a non-Fermi liquid behavior. Figure 3(c) shows the conductance in the absence of Coulomb repulsion ($U = 0$): the same effect is obtained as for the case $\alpha \neq 0$. The conductance cancellation does not depend on the electron-electron interaction, which agrees with the qualitative explanation presented below.

Figure 4 shows G as a function of V_g for different values of λ. The dip becomes more pronounced as λ increases,
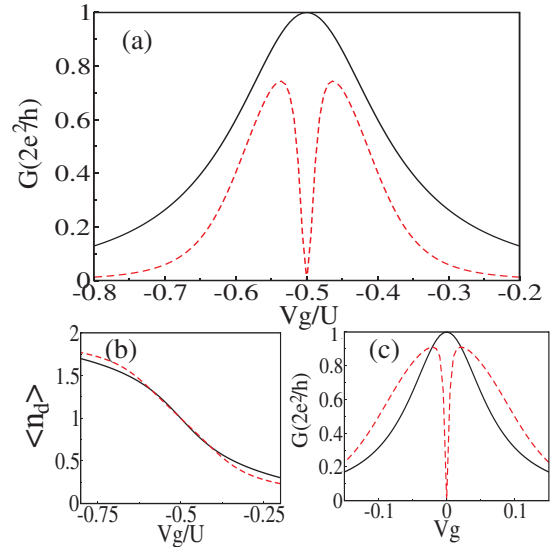

FIG. 3 (color online). (a) G vs V_g in the Kondo regime for $\alpha = 0$ (solid line) and $\alpha = 0.4$ (dashed line), $\lambda = 0.2$ in both cases. In the first case, the usual Kondo peak is obtained. In the second case, a conductance dip is obtained. (b) Average occupation for the same set of parameters. Note that the charging behavior is almost the same in both cases. (c) G vs V_g in the absence of Coulomb repulsion ($U = 0$), for $\alpha = 0$ (solid line) and $\alpha = 0.4$ (dashed line), $\lambda = 0.1$ in both cases. The dip is also obtained in this case; thus the physical mechanism behind this effect does not depend on the electron-electron interaction.
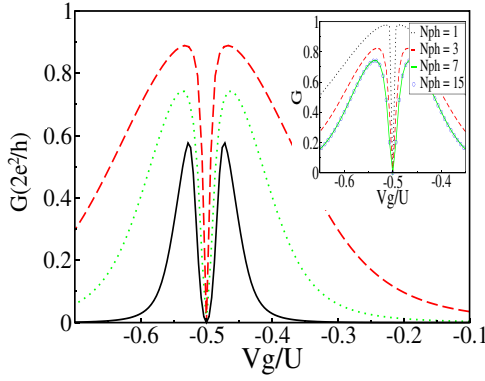
FIG. 4 (color online). G as a function of V_g in the Kondo regime for $\alpha = 0.4$ and $\lambda = 0.15, 0.20$, and 0.25 (dashed, dotted, and solid lines, respectively). The dip becomes more pronounced as λ increases. The inset shows the convergence of the results with the maximum number of phonons (N_{ph}). Note that the qualitative effect of the conductance cancellation is preserved all the way down to $N_{ph} = 1$.

i.e., as the average number of phonons in the ground state increases. The inset shows the results obtained by truncating the phonon Hilbert space at a different maximum number of phonons (N_{ph}). In all the calculations, $N_{ph} = 7$ was used unless stated otherwise. The qualitative effect of conductance cancellation is obtained all the way down to $N_{ph} = 1$, allowing us to study larger clusters and reduce size effects to intuitively understand the origin of the dip.

In Fig. 5, an explanation of the conductance dip is presented. The reasoning starts by noting that $\hat{H}_{M-\text{leads}}$ in Eq. (2) can be rewritten as a sum of two channels contributing to the overall molecule-leads connection. The first term, $t' \sum_{\sigma} (d_{\sigma}^{\dagger} c_{l0\sigma} + d_{\sigma}^{\dagger} c_{r0\sigma} + \text{H.c.})$, represents the purely electronic tunneling between the molecule and the two electrodes. The second term, $t' \alpha (a + a^{\dagger}) \sum_{\sigma} (d_{\sigma}^{\dagger} c_{r0\sigma} - d_{\sigma}^{\dagger} c_{l0\sigma} + \text{H.c.})$, represents a phonon-assisted tunneling channel, i.e., the electron absorbs (emits) a phonon upon entering the molecule and then emits (absorbs) a phonon upon leaving. Note that both channels are coherent and elastic. The number of phonons in the system does not change. Figure 5(a) shows a schematic of the two channels. These channels were studied separately by keeping only the relevant term in $\hat{H}_{M-\text{leads}}$. The conductance and the phase carried by each channel were calculated. Figure 5(b) shows the conductance of the separate channels. Figure 5(c) contains the conductance when both channels are active, i.e., when both terms are included in $\hat{H}_{M-\text{leads}}$. Figure 5(d) shows the phase difference between the two channels. Note that for $V_g = -U/2$, the conductance of each of the channels is $2e^2/h$ and the phase difference is π, leading to a perfect cancellation in the overall conductance [9]. This interference effect is independent of the electron-electron interaction and, thus, the cancellation should still be present for $U = 0$ as already shown.
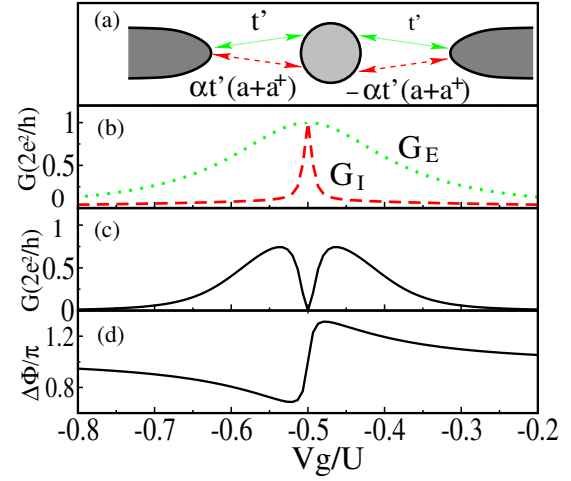

FIG. 5 (color online). (a) A schematic representation of the two conductance channels, the purely electronic tunneling represented by the two upper arrows and the "phonon-assisted tunneling" channel represented by the two lower arrows. (b) Partial conductance when only one of the channels is active. The dotted line shows the conductance of the first channel G_E, while the dashed line shows the conductance of the second channel G_I. (c) G when both channels are active. (d) Phase difference $\Delta \Phi$ of the two channels. Note that for $V_g = -U/2$, $\Delta \Phi = \pi$ and $G_E = G_I = 2e^2/h$, thus leading to a perfect cancellation in the overall conductance. ($\lambda = 0.2$, $\alpha = 0.4$.)

The stability of the dip is tested by adding an internal vibrational mode which leads to the symmetric modulation of the tunnel barriers to the leads (breathing mode). To account for this mode, the following terms were added to the Hamiltonian: $\hat{H}' = \lambda'(1 - \hat{n}_d)(b + b^{\dagger}) + \omega_0' b^{\dagger} b + t' \alpha'(b + b^{\dagger}) \sum_{\sigma} (d_{\sigma}^{\dagger} c_{l0\sigma} + d_{\sigma}^{\dagger} c_{r0\sigma} + \text{H.c.})$, where the first term represents the electron-phonon coupling, the second term represents the breathing vibrational energy, and the third term represents the subsequent modulation of the tunnel barriers. The results are shown in Fig. 6. When
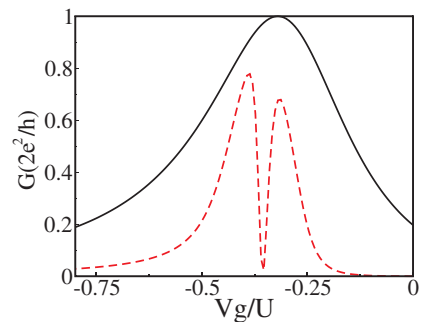

FIG. 6 (color online). The solid line shows G when a breathing vibrational mode is active (no c.m. motion). The particle-hole symmetry is broken as expected and no conductance dip is obtained. The dashed line shows G when both breathing and c.m. vibrational modes are active. The combined effects of the two modes lead to a Fano-like interference. The breathing mode parameters used are $\lambda' = 0.2$, $\omega_0' = 0.3$, and $\alpha' = 0.3$.
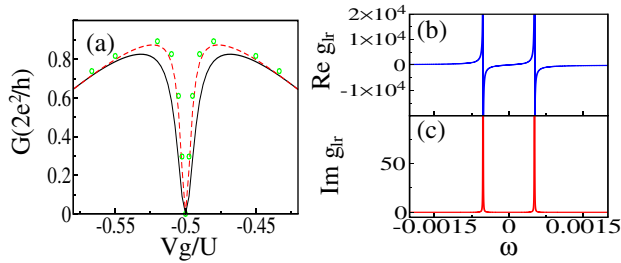
FIG. 7 (color online).   (a) Convergence of G with the size of the exactly solved cluster L. The solid line, dashed line, and the circles show the results obtained using $L = 3$, 7, and 11, respectively. In the three cases, $N_{ph} = 3$ was used. (b) The real and (c) imaginary parts of the isolated cluster Green function g_{lr} that propagates an electron from the left to the right ends of the cluster ($L = 3$ and $V_g = -U/2$). Note that both parts are equal to zero at the Fermi level (located at $\omega = 0.0$). Thus, the origin of the conductance dip can be traced back to the exactly solved cluster. $\lambda = 0.2$ and $\alpha = 0.4$ in the three figures.

only the internal mode is active (solid line), the electron-hole symmetry is broken but no dip is observed. This agrees with previous results [18] obtained using NRG calculations. In the case where both vibrational modes are active (dashed line), the dip appears. The combined effect of conductance cancellation and electron-hole asymmetry leads to a Fano-like interference.

The finite-size effects on the results are shown in Fig. 7(a), where the convergence of the conductance with the size of the exactly solved cluster is presented. Note that increasing the cluster does *not* change the qualitative effect of the conductance dip. Moreover, the origin of the conductance dip can be traced back to the exactly solved cluster by studying the Green functions *before* the embedding process. Figures 7(b) and 7(c) show the real and imaginary parts of the Green function g_{lr} that propagates an electron from the left to the right end of the cluster for $\alpha \neq 0$ and $V_g = -U/2$. Both parts are zero at the Fermi level ($\omega = 0$). For $\alpha = 0$ (not shown here), g_{lr} has a pole at the Fermi level and the system is perfectly conducting. When α is turned on, the pole splits into two, one below and one above the Fermi level thus causing the zero conductance.

In conclusion, the zero temperature electron transport through a molecular conductor with center-of-mass motion was studied numerically for interacting and noninteracting electrons. The results present an interesting conductance dip when an odd number of electrons occupy the molecule. It is argued that this dip is caused by the destructive interference between the purely electronic and phonon-assisted tunneling channels, which were found to carry opposite phases. When an internal vibrational mode is also active, the particle-hole symmetry is broken but a Fano-like interference is still obtained. The conductance

cancellation would best be observed on a broad conductance peak such as the Kondo peak, which is broader than the resonant tunneling peak.

[1] J. R. Heath and M. A. Ratner, Phys. Today **43**, No. 5, 43 (2003).

[2] C. Joachim *et al.*, Phys. Rev. Lett. **74**, 2102 (1995); M. A. Reed *et al.*, Science **278**, 252 (1997); R. H. M. Smit *et al.*, Nature (London) **419**, 906 (2002); J. Reichert *et al.*, Phys. Rev. Lett. **88**, 176804 (2002).

[3] L. I. Glazman and M. E. Raikh, Pis'ma Zh. Eksp. Teor. Fiz. **47**, 378 (1988) [JETP Lett. **47**, 452 (1988)]; T. K. Ng and P. A. Lee, Phys. Rev. Lett. **61**, 1768 (1988); Y. Meir and N. S. Wingreen, Phys. Rev. Lett. **68**, 2512 (1992); J. Paaske *et al.*, Phys. Rev. B **70**, 155301 (2004).

[4] J. Park *et al.*, Nature (London) **417**, 722 (2002); W. Liang *et al.*, Nature (London) **417**, 725 (2002); Lam H. Yu *et al.*, Nano Lett. **4**, 79 (2004).

[5] D. Goldhaber-Gordon *et al.*, Nature (London) **391**, 156 (1998); S. M. Cronenwett *et al.*, Science **281**, 540 (1998); V. Madhavan *et al.*, Science **280**, 567 (1998); J. Göres *et al.*, Phys. Rev. B **62**, 2188 (2000).

[6] H. Park *et al.*, Nature (London) **407**, 57 (2000).

[7] L. H. Yu *et al.*, Phys. Rev. Lett. **93**, 266802 (2004).

[8] A. Mitra *et al.*, Phys. Rev. B **69**, 245302 (2004), and references therein; E. Vernek *et al.*, Phys. Rev. B **72**, 121405(R) (2005).

[9] C. A. Büsser *et al.*, Phys. Rev. B **70**, 245303 (2004); T.-S. Kim and S. Hershfield, Phys. Rev. B **67**, 235330 (2003); J. L. D'Amato *et al.*, Phys. Rev. B **39**, 3554 (1989).

[10] Some results were gathered keeping up to the second order in $\hat{x}$ and the conclusions are unchanged.

[11] L. Arrachea *et al.*, Phys. Rev. B **67**, 134307 (2003).

[12] The value of U was selected to allow for the Kondo cloud to fit in our finite lattice; see C. A. Büsser *et al.*, Phys. Rev. B **62**, 9907 (2000).

[13] Yigal Meir *et al.*, Phys. Rev. Lett. **66**, 3048 (1991); E. V. Anda and F. Flores, J. Phys. Condens. Matter **3**, 9087 (1991); H. M. Pastawski, Phys. Rev. B **46**, 4053 (1992).

[14] A complete description of the method is available online (http://correlate8.phys.utk.edu/transport.pdf). This method was originally proposed by E. V. Anda and G. Chiappe. See V. Ferrari *et al.*, Phys. Rev. Lett. **82**, 5088 (1999); M. A. Davidovich *et al.*, Phys. Rev. B **65**, 233310 (2002); M. E. Torio *et al.*, Phys. Rev. B **65**, 085302 (2002); A. A. Aligia *et al.*, J. Phys. Condens. Matter **17**, S1095 (2005).

[15] P. S. Cornaglia *et al.*, Phys. Rev. Lett. **93**, 147201 (2004).

[16] A. C. Hewson and D. Meyer, J. Phys. Condens. Matter **14**, 427 (2002).

[17] A. C. Hewson, *The Kondo Problem to Heavy Fermions* (Cambridge University Press, Cambridge, England, 1997).

[18] P. S. Cornaglia *et al.*, Phys. Rev. B **71**, 075320 (2005).